26th ABCM International Congress of Mechanical Engineering
November 22-26, 2021. Florianópolis, SC, Brazil

COB-2021 1122 VISCOELASTIC MODELING OF PORCINE LIGAMENTS

Bruno Mello Silveira
Stephanie Aguiar Salles de Barros
Departamento de Engenharia Mecânica - CEFET/RJ; Av. Maracanã, 229 – RJ – Brazil. bruno.silveira@aluno.cefet-rj.br, stephanie.barros@aluno.cefet-rj.br

Rodrigo Ribeiro Pinho Rodarte
Programa de Pós-graduação em Engenharia Mecânica e Tecnologia de Materiais - PPEMM - CEFET/RJ; Av. Maracanã, 229 – RJ – Brazil. Instituto Nacional de Traumatologia e Ortopedia – INTO -Av. Brazil, 500, RJ, Brazil. rodrigo.rodarte@aluno.cefet-rj.br

Paulo Pedro Kenedi
Programa de Pós-graduação em Engenharia Mecânica e Tecnologia de Materiais - PPEMM - CEFET/RJ; Av. Maracanã, 229 – RJ – Brazil. Departamento de Engenharia Mecânica – CEFET/RJ - Av. Maracanã, 229 – RJ – Brazil. paulo.kenedi@cefet-rj.br

Abstract. *Viscoelastic quasi-linear analytical models, as Fung, was implemented through the utilization of experimental results obtained from several porcine ligaments experimental tests as: lateral collateral ligament (LCL), anterior cruciate ligament (ACL), posterior cruciate ligament (PCL) and medial collateral ligament (MCL). To implement quasi-linear viscoelastic models for soft tissues, as the Fung one, it was necessary the utilization of a programming language, as C Sharp, and Object-oriented programming to deal with the model's mathematical demands, as the convolution calculations. Moreover, those technologies allow to reduce the code execution time, which was one of the main challenges. The numerical implementation of Fung's model successfully reproduced the stress evolution in relaxation tests.*

Keywords: *knee ligaments, numerical model, viscoelasticity, Fung's model*

1. INTRODUCTION

The knee is one of the most complex joints of the body. The description of the mechanical behavior of the knee ligaments is an essential requirement to the implementation of knee mechanical models. Thus, several research have been published attempting to macroscopically analyze the knee ligaments/tendons through the application of several viscoelastic mechanical models. (Rossetto *et al*., 2013) shows that this knowledge was important to improve the decisions in relation to physical training, such as in cases of therapy for tendinopathies. (Bernardes *et al.*, 2005) sought to determine the biomechanical parameters for modeling the human knee joint submitted to extensive exercises. They used images, obtained by videofluoroscope, to access the ligaments viscoelasticity.

Viscoelasticity is understood as the property of materials that present viscous and elastic behavior at the same time. This concept is widely used by numerous areas. The simplest viscoelastic model is the one that considers linear functions, where the creep compliance and stress relaxation functions depends only on the time. This approach is commonly used for metals. (Tareco, 2014) uses Maxwell and Kelvin linear models to design steel-concrete structures, analyzing the relaxation and creep compliance, just for the concrete, in the mixed structure response. Moreover, as presented by (Queiroz, 2008), viscoelastic materials are also used to attenuate vibrations and noise of structures having application, in both, automotive and aerospace sectors.

The quasi-linear viscoelastic model, proposed by (Fung, 1993), is frequently used to describe the soft tissues' behavior. (Piazza *et al.*, 2001) had developed a three-dimensional dynamic model of a tibiofemoral and patellofemoral articulations, to predict the knee implant movements during a step-up activity. They were based on the Fung's model, using dynamic equations of motion subjected to forces generated by muscles, ligaments, and contact articulations. They achieved good results for the knee flexion-extension angle, but not for translations at the tibiofemoral articulations. (Abramowitch *et al.*, 2004b) applied the Fung's model to investigate the viscoelastic properties of a healing goat MCL. They characterized the reduced relaxation function and the elastic response. They demonstrated that the quasi-linear viscoelastic model could be successfully used to describe the analyzed ligament viscoelastic behavior, during the healing phase.

Moreover, the quasi-linear viscoelastic method is frequently employed with computational resources, since it has complex equations and doesn't have any available explicit analytical solution. (Xu and Engquist, 2018) proposed a mathematical model for relaxation modulus based on nonlinear model and its numerical solution. They developed a finite-

element framework and a numerical algorithm to implement this model for simulating responses, under static and dynamic loadings. They validated their model through the utilization of various materials, comparing experimental and numerical results. (Weiss and Gardiner, 2001) reviewed earlier and current techniques for the computational modeling of soft tissues, showing relevant concepts under the perspective of continuum mechanics and finite element method. Also, emphasized the microstructural influence of soft tissues. (Abramowitch *et al.*, 2004a) obtained the constants for quasi-linear viscoelastic model that was used to describe the elastic response, with constants A and B, and the reduced relaxation function, with constants C, τ_1 and τ_2. They subjected six goat femur-MCL-tibia to uniaxial tension tests, considering the ramp time. In those tests, the convergence had failed for three ligaments, with the biggest errors were found for constants A, B e τ_1.

The aim of this paper is to describe the numerical implementation of the Fung's quasi-linear viscoelasticity model. To achieve this goal, the C# programming language was utilized, as in (Wagner *et al.*, 2021) in conjunction with a ASP.NET MVC framework, as in (Rick Anderson, 2019) and (Gasparotto, 2014). (Silveira, 2020) had developed a REST API, which could perform the necessary calculations and generating a CSV file, which, in turn, was used to compare the numerical and experimental results. Furthermore, the main advantage of the API is having a complete tool set, which meet the research's necessities of systematizing the repetitive work. Also, it was focused on scalability, maintainability, and readability, through the utilization of object-oriented programming patterns, as SOLID principles. Some resources were, also, used to optimize the software performance, as Swagger, for building the user interface.

2. FUNG'S QUASI-LINEAR VISCOELASTIC MODEL

The quasi-linear viscoelastic model, (Fung, 1993), was proposed with a non-linear stress-strain relation, divided in two parts: the reduced relaxation function, which depends only on time, and the elastic response, which depends on strain. The Fung's model was originally proposed as a tensorial, more general, version. (Weiss and Gardiner, 2001) considered that in case of the animal ligaments the strains and the rotations were small. So, the linear strain (infinitesimal) could be used in Fung's model, as an 1D scalar version. In fact, this model is commonly used for soft tissue, with good performance. It is based on Boltzmann superposition principle, which stated that the contribution of each strain to the stress relaxation of the ligament is treated as being independent of each other. The total stress of the ligament is approximated by the linear summation of all the previous stresses.

(Fung, 1993) propose equations for elastic response, reduced relaxation function and stress considering one relaxation. For two relaxations, in sequence, considered in this paper, it was necessary to adapt these equations. Moreover, each parameter will be expressed accordingly, for considering or disregarding ramp time, except for the reduced relaxation function.

Strain and strain rate application

The equations used to describe the imposed strains were developed to represent the experiments. Considering the ramp time, the strain behavior is expressed by equation (1). While the strain stays at the maximum value ε_{max}, the stresses show the relaxation behavior. When the strain stays at the minimum value ε_{min}, the stresses show the recovery behavior. These behaviors were also observed in (Duenwald *et al.*, 2009). While disregarding ramp time, the equation (2) can be used, where it is considered a constant strain during the whole experiment.

$$\varepsilon(t) = \begin{cases} \lambda_1 \cdot t, & 0 \le t < t_0 \\ \varepsilon_{max}, & t_0 \le t < t_1 \\ \varepsilon_{max} - \lambda_2 \cdot (t - t_1), & t_1 \le t < t_2 \\ \varepsilon_{min}, & t_2 \le t < t_3 \\ \varepsilon_{min} + \lambda_1 \cdot (t - t_3), & t_3 \le t < t_4 \\ \varepsilon_{max}, & t \ge t_4 \end{cases}, \tag{1}$$

Where, the parameters t_0 and λ represent, respectively, ramp time and strain rate applied to the experiment, with λ_1 used when strain is increasing and λ_2, when the strain is decreasing. Furthermore, the parameters t_1, t_2, t_3 and t_4 are the time limits for each equation, indicating when the strain behavior changes.

$$\varepsilon(t) = \varepsilon_0, \tag{2}$$

where, ε_0 represents the constant strain applied through the whole experiment.

It is possible to calculate the derivative that will be used in the stress calculations step. The equations (3) and (4) are the time derivative of, respectively, equations (1) and (2).

$$\frac{d\varepsilon(t)}{dt} = \begin{cases} \lambda_1, & 0 \le t < t_0 \\ 0, & t_0 \le t < t_1 \\ -\lambda_2, & t_1 \le t < t_2 \\ 0, & t_2 \le t < t_3 \\ \lambda_1, & t_3 \le t < t_4 \\ 0, & t \ge t_4 \end{cases} \tag{3}$$

$$\frac{d\varepsilon(t)}{dt} = 0 \tag{4}$$

Fig. 1 show the graphical representation of equations (1) and (3).

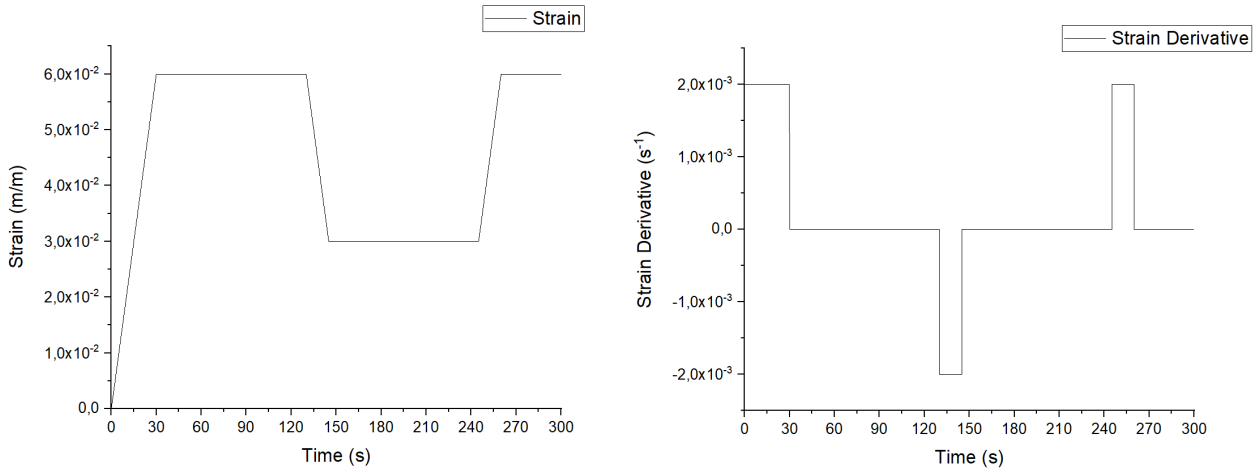

(a) (b)

Figure 1. (a) Strain vs time and (b) strain derivative vs time.

Note that, in Fig.1.a, the minimum and maximum strain applied in experiment are, respectively, $\varepsilon_{min} = 3 \cdot 10^{-2}\ m/m$ and $\varepsilon_{max} = 6 \cdot 10^{-2}\ m/m$, and the strain rate used in ramp time and descent time are $\lambda_1 = -\lambda_2 = 2 \cdot 10^{-3}\ s^{-1}$.

Elastic stress response

The elastic response corresponds to a portion of Fung's model. When considering ramp time, an exponential approximation can be used like that proposed by (Abramowitch *et al*., 2004a):

$$\sigma_e(\varepsilon) = A \cdot (e^{B\varepsilon} - 1) \tag{5}$$

Where constants *A*, in MPa, and *B*, dimensionless, are material constants. They represent, respectively, an elastic stress constant and an elastic power constant. Moreover, as shown previously, the equation (5) can be rewritten with only time dependence.

$$\sigma_e(t) = A \cdot \left(e^{B\varepsilon(t)} - 1\right) \tag{6}$$

The elastic derivative response must be calculated to be used for the description of the stress evolution. The derivative, in strain and in time are, respectively:

$$\frac{d\sigma_e(\varepsilon)}{d\varepsilon} = A \cdot B \cdot e^{B\varepsilon} \tag{7}$$

$$\frac{d\sigma_e(t)}{dt} = A \cdot B \cdot e^{B\varepsilon(t)} \cdot \frac{d\varepsilon(t)}{dt} \tag{8}$$

When ramp time is disregarded, the elastic response is considered constant for all time domain.

$$\sigma_e(\varepsilon) = \sigma_e(t) = \sigma_0 \tag{9}$$

Where, σ_0 is the initial stress applied in the experiment. The derivative in time and in strain for equation (9) is:

$$\frac{d\sigma_e(\varepsilon)}{d\varepsilon} = \frac{d\sigma_e(t)}{dt} = 0 \tag{10}$$

Reduced relaxation function

The reduced relaxation function represents the viscous part of Fung's model. It occurs for the entire time domain, with g(0) = 1. (Fung, 1993) stated that it can be described in two ways. The first one, shown in the equation (11), also called the simplified reduced relaxation function. It is written using the first three Prony Series (Babaei *et al.*, 2015). Also, (Funk *et al.*, 2000) stated that more than three elements do not result in any significant gain. The second way, shown in the equation (12), was developed after Kelvin model, standard linear solid. It uses integrals that only have numerical solutions. Moreover, both equations were implemented and tested in this research, but only the first one was effectively used, as their constants are easier to be calculated experimentally.

$$g(t) = G_\infty + \sum_{i=1}^{3} G_i \cdot e^{\frac{-t}{\tau_i}} \tag{11}$$

where G_∞ and G_i are material dimensionless constants called relaxation modulus and represents the amplitude of the stress curve in relaxation, and τ_i is the relaxation time in seconds, also a material constant.

$$g(t) = \frac{1 + C \cdot \left[E_1\left(\frac{t}{\tau_2}\right) - E_1\left(\frac{t}{\tau_1}\right)\right]}{\left[1 + C \cdot \ln\left(\frac{\tau_2}{\tau_1}\right)\right]} \qquad where\ E_1(z) = \int_z^\infty \frac{e^{-x}}{x} dx \tag{12}$$

where C, τ_1 and τ_2 are material constants and represents, respectively, a dimensionless relaxation constant, fast and slow relaxation times in seconds. The equation (12) can be rewritten, with the development shown in Appendix:

$$g(t) = \frac{1 + C \cdot I(t)}{1 + C \cdot \ln\left(\frac{\tau_2}{\tau_1}\right)} \qquad where\ I(t) = \int_{\frac{t}{\tau_2}}^{\frac{t}{\tau_1}} \frac{e^{-x}}{x} dx \tag{13}$$

Also calculating the derivative with respect to time of equation (13), for reduced relaxation function, in Appendix:

$$\frac{dg(t)}{dt} = \frac{C}{1 + C \cdot \ln\left(\frac{\tau_2}{\tau_1}\right)} \cdot \frac{e^{-\left(\frac{t}{\tau_1}\right)} - e^{-\left(\frac{t}{\tau_2}\right)}}{t} \tag{14}$$

(Fung, 1993) shows that three equivalent equations can be used to calculate the stresses:

$$\sigma(t) = \sigma_e(0) \cdot g(t) + \int_0^t g(t-\tau) \frac{\partial \sigma_e(\tau)}{\partial \tau} d\tau \tag{15}$$

$$\sigma(t) = \sigma_e(t) \cdot g(0) + \int_0^t \sigma_e(t-\tau) \cdot \frac{\partial g(\tau)}{\partial \tau} d\tau \tag{16}$$

$$\sigma(t) = \frac{\partial}{\partial t} \int_0^t \sigma_e(t-\tau) \cdot g(\tau) d\tau \tag{17}$$

As mentioned previously, the elastic response and reduced relaxation function can be expressed only in function of time, so the partial derivative can be changed to total derivative. Moreover, $\sigma_e(0) = 0$ and $g(t) = 1$.

$$\sigma(t) = \int_0^t g(t-\tau) \cdot \frac{d\sigma_e(\tau)}{d\tau} d\tau \tag{18}$$

$$\sigma(t) = \sigma_e(t) + \int_0^t \sigma_e(t-\tau) \cdot \frac{dg(\tau)}{d\tau} d\tau \tag{19}$$

$$\sigma(t) = \frac{d}{dt} \int_0^t \sigma_e(t-\tau) \cdot g(\tau) d\tau \tag{20}$$

Considering ramp time, all equations return satisfactory results. Disregarding ramp time, the elastic response is constant, and its derivative is zero for all time domain, as shown previously. Thus, the equation (18) cannot be used, because it always returns zero, and equations (19) and (20) can be rewritten. As shown in Appendix, equations (19) and (20) return to the same expression, shown in equation (21). So, when disregarding the ramp time, a unique equation can be used:

$$\sigma(t) = \sigma_e \cdot g(t) \tag{21}$$

Fig. 2.a shows the graphical representation of equations (18-20) and equivalently in Fig. 2.b for equation (21).

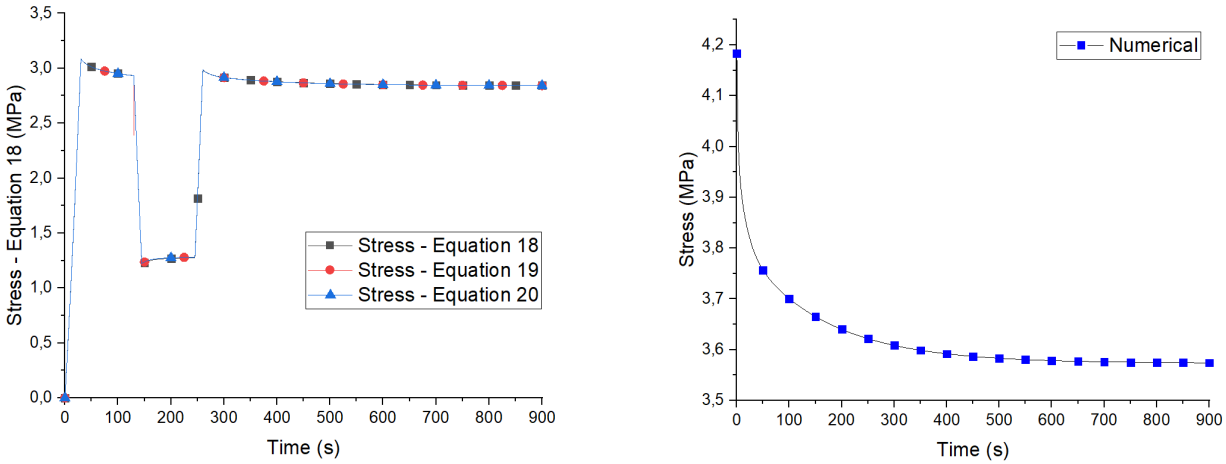

(a) (b)

Figure 2. Stress vs time using: (a) equations (18-20) and (b) equation (21).

The equations (15-21) are in scalar form. In the next section the numerical implementation of the Fung's equations will be fully explained.

3. NUMERICAL IMPLEMENTATION

The numerical implementation of Fung's model was developed in two steps: a) creating a class that represents the model, which contains the equations for each parameter and its respective derivative in time; and b) creating a class to orchestrate the operation. Also, it was created an artificial frontier, in the code, that separates the operation and the model, creating specific contracts for each one. It was done based on Single-Responsibility Principle that gets easier to implement resources, prevents unexpected side effects and improves maintainability. To improve numerical implementation performance, it was used the class Task, a native resource from C#. The objective was to process some steps asynchronously, executing multiple tasks together and reducing the execution time

In Fig. 3 shows the flowchart for main operation, that calculates the results for Fung's model and the respective sub-routine. The class that represents the model also contains a method, represented in Fig. 3 as sub-routine "Calculate Results". It calculates, in parallel, all results necessaries - strain, elastic response, reduced relaxation function and stress as shown in Fig. 3.b, returning those values in an object. The orchestrator is responsible to validate the request data and, if it is valid, execute each step shown in Fig. 3.a.

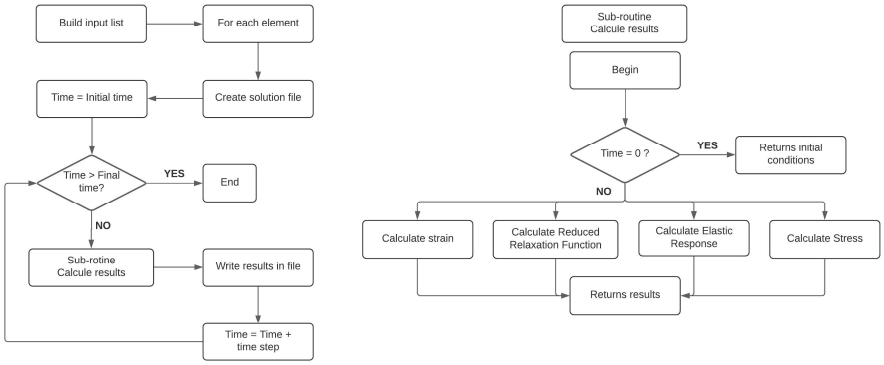

(a) (b)

Figure 3. Flowchart for (a) main operation and (b) sub-routine “Calculate Results”.

It also was necessary to implement numerical methods to deal with integrations and derivatives present in stress and reduced relaxation function equations. For the integrals, it was used the Composite Simpson's Rule, stated in equation (22), available in (Regra de Simpson, 2021) (Regras Compostas, 2021). For the derivatives, it was used the Symmetric Derivative, stated in equation (23), available in (da Cruz, 2012).

$$\int_a^b f(x)dx = \frac{\Delta x}{3}\left[f(x_0) + 4\cdot\sum_{k=1}^{N/2} f(x_{2k-1}) + 2\cdot\sum_{k=1}^{(N/2)-1} f(x_{2k}) + f(x_N)\right] \tag{22}$$

where f(x) is an integrable function, a and b are the limits of integration, Δx is an interval of the variable x, and N is the number of subdivisions.

$$\frac{df(x)}{dx} = \frac{f(x+\Delta x) - f(x-\Delta x)}{2\Delta x} \tag{23}$$

where f(x) is a differentiable function.

Numerical extrapolation

Furthermore, for a better comparison with experimental results, it was necessary to develop a routine to extrapolating the experimental results. To implement this, it was necessary to predict the next values based on the earlier stress curves' behavior. Considering that during relaxation there are two important behaviors occurring: the stress decreases with time and the concavity has upwards direction. These typical behaviors were used to validate each point, before applying extrapolation, and to remove invalid points that could interfere in the final extrapolated results.

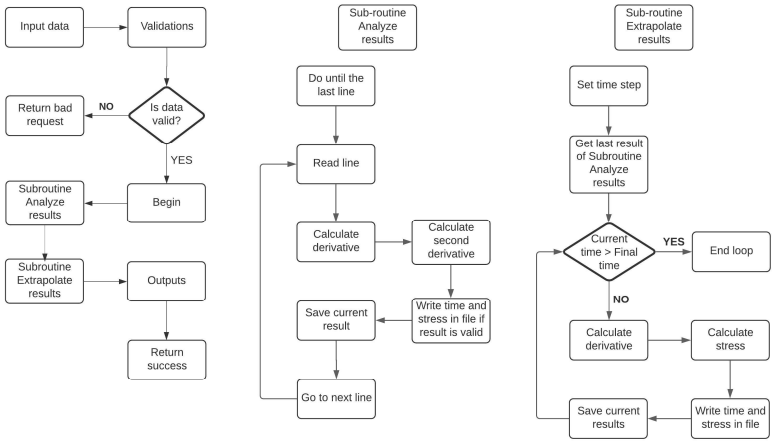

Figure 4. Flowchart for numerical extrapolation.

The numerical extrapolation was made according to the flowchart of Fig. 4. The operation was divided in two subroutines to improve maintainability and readability. It’s worth mentioning that after the API receives input data, these are validated to ensure that the file has enough lines for the operation.

4. RESULTS AND CONCLUSIONS

The obtained numerical results essentially overlap the experimental ones. Fig. 5 shows the comparison between these values, when disregarding the ramp time. This hypothesis is in line with the consideration proposed in the Fung's model, where it is assumed that the initial stress must be applied as fast as a step. These graphs are equivalent to the ones shown in Fig.2.b.

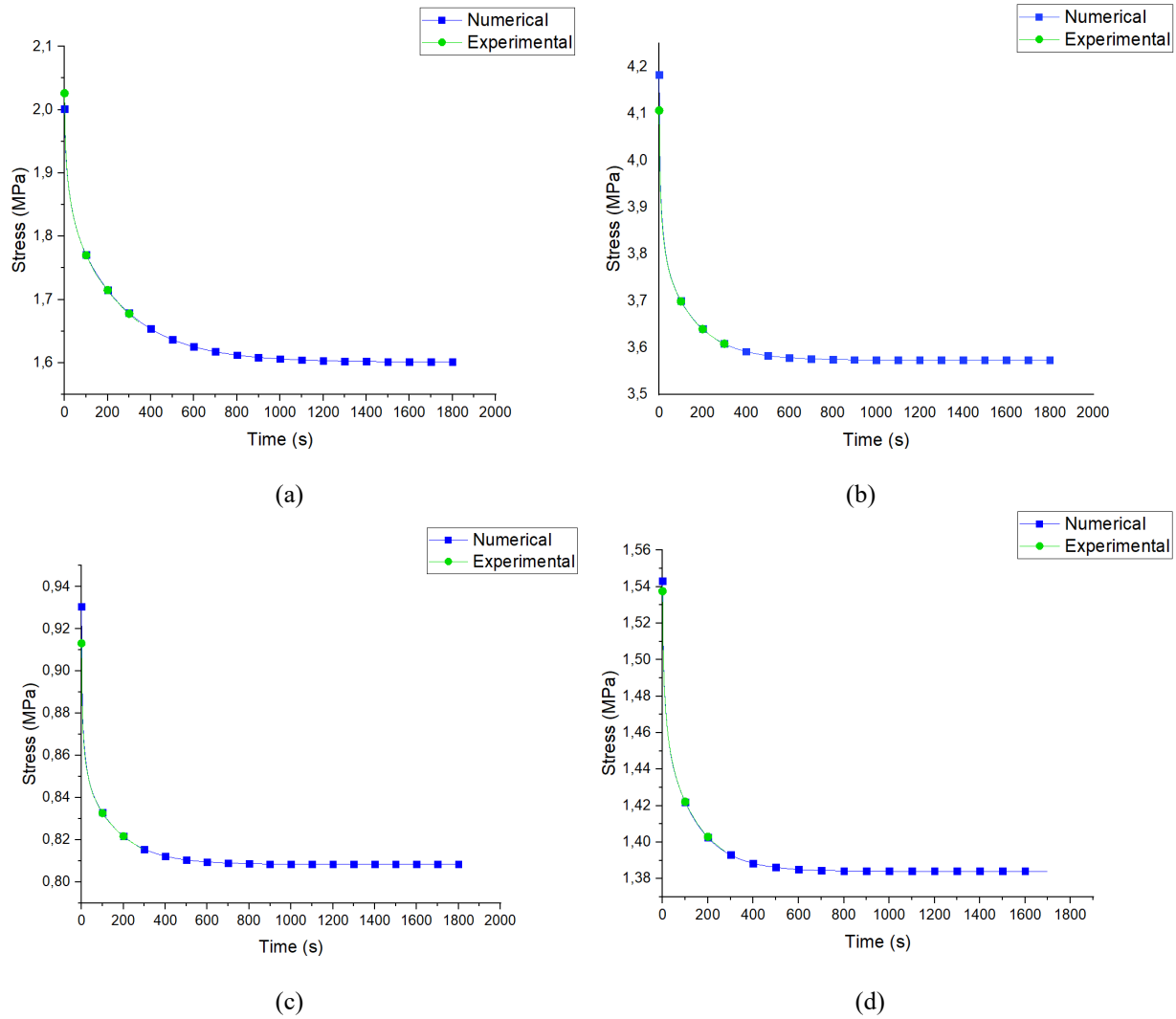

Figure 5. Stress vs time for (a) ACL, (b) LCL, (c) MCL and LCP. (The the experimental results were obtained by the biomechanics CEFET/RJ's research group)

As shown in Fig. 5, it was possible to reproduce the experimental behavior using the Fung's model equations. The first part of these graphics (green points), the experimental and the numerical points are directly compared (up to about 300 s). Thenceforth the points are just numerical (blue points), from extrapolation calculations.

The numerical implementation of the Fung's model was quite successful. All step, both mathematical and software implementation, were fully covered by this text. Beyond the reliable reproduction of experimental results, the extrapolation of the relaxation experimental data (blue points), up to an asymptotic behavior, proved to be consistent. This text covers the numerical part of an extensive research about the porcine ligaments mechanical characterization, with focus in their viscoelastic behavior. With the development of this research, the porcine ligaments experimental/numerical results can be utilized, for instance, as a preliminary step, to contribute to the increase the knowledge about the mechanical performance of human knees ligaments.

5. ACKNOWLEDGEMENTS

Bruno Mello Silveira and Stephanie Aguiar Salles de Barros are grateful for scholarship granted by CNPq.

6. REFERENCES

Abramowitch, S.D. and Woo, S.L.Y., 2004a. “An Improved Method to Analyze the Stress Relaxation of Ligaments Following a Finite Ramp Time Based on the Quasi-Linear Viscoelastic Theory”. *Journal of Biomechanical Engineering*. ASME. Vol. 126., pp. 92-97. DOI: 10.1115/1.1645528.

Abramowitch, S.D; Woo, S.L.Y.; Clineff, T. D. and R.E., Debski, 2004b. “An evaluation of the quasi-linear viscoelastic properties of the healing medial collateral ligament in a goat model”. *Annals of Biomedical Engineering*. Vol. 32, No. 3, pp. 329-335. DOI: 10.1023/b:abme.0000017539.85245.6a.

Babaei, Behzad, et al. 2015. “Efficient and optimized identification of generalized Maxwell viscoelastic relaxation spectra”. *Journal of the Mechanical Behavior of Biomedical Materials*. Vol. 55, pp. 32-41. Available in: http://dx.doi.org/10.1016/j.jmbbm.2015.10.008. Accessed on May 6, 2021.

Bernardes, C., et al. 2005. “Biomechanical parameters' determination for knee joint modeling”. Laboratório de Pesquisa do Exercício, Universidade Federal do Rio Grande do Sul. Porto Alegre.

da Cruz, A. M.C. B., Martins, N., Torres, D. F.M. 2012. “Symmetric differentiation on time scales”. *Applied Mathematics Letters*, Vol. 60, No. 2, pp. 264-269. DOI:10.1016/j.aml.2012.09.005.

Duenwald, S. E.; Jr., R. V.; Lakes, R. S., 2009. “Viscoelastic Relaxation and Recovery of Tendon”. *Annals of Biomedical Engineering*. Vol. 37, No. 6, pp. 1131–1140. DOI: 10.1007/s10439-009-9687-0.

Fung, Y. 1993. “Biomechanics: Mechanical Properties of Living Tissues”. Springer, New York, University of Michigan.

Funk, J. R., Hall, G. W., Crandall, J. R., Pilkey, W. D., 2000. “Linear and quasi-linear viscoelastic characterization of ankle ligaments”. Journal of Biomechanical Engineering, Vol. 122, No. 1, pp. 15-22. DOI:10.1115/1.429623.

Gasparotto, H. M. 2014. “ASP.NET MVC Introduction”. DEVMEDIA. 2014. Available in: devmedia.com.br/introducao-ao-asp-net-mvc/31878. Accessed on June 19, 2021.

Piazza, Stephen J.; Delp, Scott L. 2001. “Three-Dimensional Dynamic Simulation of Total Knee Replacement Motion During a Step-Up Task”. *Journal of Biomechanical Engineering*. ASME. Vol. 123. pp. 599-606. DOI: 10.1115/1.1406950.

Queiroz, José Aparecido Silva de. 2008. “Flexible structures analysis with viscoelastic materials application”. Universidade Estadual Paulista, Faculdade de Engenharia de Bauru, 2008. Available in: https://repositorioslatinoamericanos.uchile.cl/handle/2250/2568006. Accessed on May 4, 2021.

Regra de Simpson. Instituto Superior Técnico de Lisboa. Available in: https://www.math.tecnico.ulisboa.pt/.Accessed on: May 18, 2021.

Regras Compostas. Universidade Federal do Rio Grande do Sul. Available in: https://www.ufrgs.br/reamat/CalculoNumerico/livro-oct/in-regras_compostas.html. Accessed on May 18, 2021.

Rick Anderson. 2019. “ASP.NET overview”. Microsoft. Available in: https://docs.microsoft.com/en-us/aspnet/overview. Accessed on June 19, 2021.

Rossetto, N.P., dal Fabbro, I.M. and Piedade, S.R. 2013. “How does static stretching influence the tendons mechanical response?”. *Acta ortop. bras*. Vol. 21, No.5. DOI: 10.1590/S1413-78522013000500003.

Silveira, B. M. 2020. “SoftTissue”. Available in: https://github.com/M3110/SoftTissue. Accessed on June 01, 2021.

Tareco, M. A. C. 2014. Conceitos de viscoelasticidade na modelação da fluência em estruturas mistas aço-betão. 154f. Dissertação (Mestrado) – Engenharia Civil, Faculdade de Ciências e Tecnologia. Lisboa, 2014. Available in: https://run.unl.pt/bitstream/10362/12481/1/Tareco_2014.pdf. Accessed on May 4, 2021.

Wagner, B., et al. 2021. “A tour of the C# language”. Microsoft. Available in: https://docs.microsoft.com/en-us/dotnet/csharp/tour-of-csharp/. Accessed on: June 14, 2021.

Weiss, J.A. and Gardiner, J.C. 2001. “Computational Modeling of Ligament Mechanics”. *Critical Reviews in Biomedical Engineering*, Vol. 29, No.4, pp. 303-371. DOI: 10.1615/CritRevBiomedEng.v29.i3.20.

Xu, Qinwu e Engquist, Björn. 2018. “A mathematical model for fitting and predicting relaxation modulus and simulating viscoelastic responses”. *Proceedings of the Royal Society A: Mathematical, Physical and Engineering Sciences*. *Proc. R. Soc. A* Vol. 474: 20170540. DOI: 10.6084/m9.figshare.c.4088969.

7. APPENDIX

7.1 Development from equation (12) to equation (13)

Based on material properties and the constants definition, it can be assumed that $\tau_2 > \tau_1$, so, $\frac{t}{\tau_2} < \frac{t}{\tau_1}$, therefore, $E_1\left(\frac{t}{\tau_2}\right)$ could be rewritten:

$$E_1\left(\frac{t}{\tau_2}\right) = \int_{\frac{t}{\tau_2}}^{\infty} \frac{e^{-x}}{x} dx = \int_{\frac{t}{\tau_2}}^{\frac{t}{\tau_1}} \frac{e^{-x}}{x} dx + \int_{\frac{t}{\tau_1}}^{\infty} \frac{e^{-x}}{x} dx \tag{i}$$

$$E_1\left(\frac{t}{\tau_2}\right) - E_1\left(\frac{t}{\tau_1}\right) = \int_{\frac{t}{\tau_2}}^{\frac{t}{\tau_1}} \frac{e^{-x}}{x} dx + \int_{\frac{t}{\tau_1}}^{\infty} \frac{e^{-x}}{x} dx - \int_{\frac{t}{\tau_1}}^{\infty} \frac{e^{-x}}{x} dx = \int_{\frac{t}{\tau_2}}^{\frac{t}{\tau_1}} \frac{e^{-x}}{x} dx \tag{ii}$$

Applying equation (ii) in (12):

$$g(t) = \frac{1+C\cdot I(t)}{1+C\cdot\ln\left(\frac{\tau_2}{\tau_1}\right)} \qquad with\ I(t) = \int_{\frac{t}{\tau_2}}^{\frac{t}{\tau_1}} \frac{e^{-x}}{x} dx, \tag{13}$$

7.2 Development from equation (13) to equation (14)

Deriving (13) in function of time:

$$\frac{dg(t)}{dt} = \frac{d}{dt}\left[\frac{1+C\cdot I(t)}{1+C\cdot\ln\left(\frac{\tau_2}{\tau_1}\right)}\right] = \frac{C}{1+C\cdot\ln\left(\frac{\tau_2}{\tau_1}\right)} \cdot \frac{d}{dt}[I(t)],\ \ where\ \frac{d}{dt}[I(t)] = \frac{d}{dt}\left[\int_{\frac{t}{\tau_2}}^{\frac{t}{\tau_1}} \frac{e^{-x}}{x} dx\right], \tag{iii}$$

Applying the definition of calculus to the derivative of a definite integral:

$$\frac{d}{dt}\int_b^a f(x)dx = \frac{d}{dt}[F(a) - F(b)] = f(a)\cdot\frac{da}{dt} - f(b)\cdot\frac{db}{dt}, \tag{iv}$$

where $f(x) = \frac{e^{-x}}{x}$, $a = \frac{t}{\tau_1}$ and $b = \frac{t}{\tau_2}$.

$$\frac{d}{dt}\left[\int_{\frac{t}{\tau_2}}^{\frac{t}{\tau_1}} \frac{e^{-x}}{x} dx\right] = \frac{e^{-\frac{t}{\tau_1}}}{\frac{t}{\tau_1}} \cdot \frac{d}{dt}\left(\frac{t}{\tau_1}\right) - \frac{e^{-\frac{t}{\tau_2}}}{\frac{t}{\tau_2}} \cdot \frac{d}{dt}\left(\frac{t}{\tau_2}\right) = \frac{e^{-\frac{t}{\tau_1}}}{\frac{t}{\tau_1}} \cdot \frac{1}{\tau_1} - \frac{e^{-\frac{t}{\tau_2}}}{\frac{t}{\tau_2}} \cdot \frac{1}{\tau_2} = \frac{e^{-\frac{t}{\tau_1}} - e^{-\frac{t}{\tau_2}}}{t}, \tag{v}$$

Applying (v) in (iii):

$$\frac{dg(t)}{dt} = \frac{C}{1+C\cdot\ln\left(\frac{\tau_2}{\tau_1}\right)} \cdot \frac{e^{-\frac{t}{\tau_1}} - e^{-\frac{t}{\tau_2}}}{t}, \tag{14}$$

7.3 Development from equation (19) and (20) to equation (21)

Rewriting (19):

$$\sigma(t) = \sigma_e + \int_0^t \sigma_e \cdot \frac{dg(\tau)}{d\tau} d\tau = \sigma_e + \sigma_e \cdot \int_0^t \frac{dg(\tau)}{d\tau} d\tau,$$

$$\sigma(t) = \sigma_e + \sigma_e \cdot \big(g(t) - g(0)\big) = \sigma_e + \sigma_e \cdot (g(t) - 1),$$

$$\sigma(t) = \sigma_e \cdot g(t). \tag{21}$$

Rewriting (20):

$$\sigma(t) = \frac{d}{dt}\int_0^t \sigma_e \cdot g(\tau) d\tau = \sigma_e \cdot \frac{d}{dt}\int_0^t g(\tau) d\tau,$$

$$\sigma(t) = \sigma_e \cdot g(t). \qquad \text{(repeated)} \qquad (21)$$

8. RESPONSIBILITY NOTICE

The authors are the only responsible for the printed material included in this paper.